# Chronometric investigations of the Middle to Upper Palaeolithic Transition in the Zagros Mountains using AMS radiocarbon dating and Bayesian age modelling

Lorena Becerra-Valdivia[a], Katerina Douka[a], Daniel Comeskey[a], Behrouz Bazgir[b,c], Nicholas J. Conard[d], Curtis W. Marean[e,f], Andreu Ollé[b,c], Marcel Otte[g], Laxmi Tumung[b,c,h], Mohsen Zeidi[d], Thomas F. G. Higham[a]

[a] Research Laboratory for Archaeology and the History of Art, University of Oxford, Dyson Perrins Building, South Parks Road, OX1 3QY Oxford, United Kingdom

[b] IPHES, Institut Català de Paleoecologia Humana i Evolució Social, Zona Educacional 4, Campus Sescelades URV (Edifici W3), 43007 Tarragona, Spain

[c] Area de Prehistoria, Universitat Rovira i Virgil. Fac. de Lletres, Av. Catalunya 35, 43002 Tarragona, Spain

[d] Abteilung Ältere Urgeschichte und Quartärökologie & Senckenberg Center for Human Evolution and Paleoenvironment (HEP), Eberhard Karls Universität Tübingen, Burgsteige 11, 72070 Tübingen, Germany, & Tübingen Senckenberg Center for Human Evolution and Paleoenvironment

[e] Institute of Human Origins, School of Human Evolution and Social Change, PO Box 872402, Arizona State University, Tempe, AZ 85287-2402, USA

[f] Centre for Coastal Palaeoscience, Nelson Mandela Metropolitan University, Port Elizabeth, Eastern Cape 6031, South Africa

[g] Service de Préhistoire, Université de Liège, 7, place du XX août, bât. A1, 4000 Liège, Belgium

[h] Histoire Naturelle de l'Homme Préhistorique (HNHP, UMR 7194), Sorbonne Universités, Muséum national d'Histoire naturelle, CNRS, Université Perpignan Via Dominica, 1 rue René Panhard, 75013 Paris, France

Corresponding author: Lorena Becerra-Valdivia (lorena.becerravaldivia@arch.ox.ac.uk)

## Abstract

The Middle to Upper Palaeolithic transition is often linked with a bio-cultural shift involving the dispersal of modern humans outside of Africa, the concomitant replacement of Neanderthals across Eurasia, and the emergence of new technological traditions. The region encompassed by the Zagros Mountains assumes importance in discussions concerning this period as its geographic location is central to all pertinent hominin migration areas, pointing to both east and west. As such, the establishment of a reliable chronology in the Zagros Mountains is crucial to our understanding of these biological and cultural developments. Political instability coupled with the poor preservation of organic material has meant that a clear chronological definition of the Middle to Upper Palaeolithic transition for the Zagros Mountains region has not yet been achieved. To improve this situation, we have obtained new archaeological samples for AMS radiocarbon dating from three sites: Kobeh Cave, Kaldar Cave, and Ghār-e Boof (Iran). In addition, we have statistically modelled previously published radiocarbon determinations for Yafteh Cave (Iran) and Shanidar Cave (Iraqi Kurdistan), to improve their chronological resolution and enable us to compare the results with the new dataset. Bayesian modelling results suggest that the Middle to Upper Palaeolithic transition in the Zagros Mountains dates to 45,000-40,250 cal BP (68.2% probability). Further chronometric data is required to improve the precision of this age range.

Keywords: AMS radiocarbon dating; Bayesian age modelling; Zagros Mountains; Upper Palaeolithic; Middle Palaeolithic

## 1. Introduction

The Middle to Upper Palaeolithic (M-UP) transition, dating to between 45,000 and 35,000 years Before Present (BP), marks a pivotal point in late human evolution. It involves the dispersal of anatomically modern humans (AMHs) outside of Africa, the concomitant replacement of Neanderthal populations across the Eurasian record, and the emergence of what is widely termed the 'Early Upper Paleolithic' (EUP)—a

period often associated with novel symbolic and behaviourally mediated artefacts thought to represent an important change in the cognitive processes of modern humans (see White et al., 1982; Mellars, 1991; Klein, 1995; Bar-Yosef, 2002 ). It is axiomatic that a reliable chronology is required to allow us to compare archaeological sites and material culture across space and place the biological and cultural developments occurring at this time in a proper context. So far, however, the vast majority of Palaeolithic archaeological sites that have been investigated chronometrically in any great detail are in Europe. Elsewhere, as is the case with the Zagros Mountains, the archaeological record is not only less abundant, but chronometric data is often absent. Considering that this geographic region acts as a corridor linking Africa to the Levant and Eurasia, establishing a spatio-temporal sequence for the Zagros is crucial. Due to political instability within the region and the poor preservation of organic material (bone collagen, in particular) extracted from archaeological sites, however, a clear chronological definition for the M-UP transition has not yet been achieved—very few absolute dates have been published (e.g., Solecki, 1963; Conard and Ghasidian, 2011; Otte et al., 2011; Heydari-Guran and Ghasidian, 2017). In this article, we present new accelerator mass spectrometry (AMS) radiocarbon results from three archaeological sites in the Zagros Mountains and model chronometric data using Bayesian statistics.

## 2. Background

### *2.1. Neanderthals and AMHs*

Neanderthals and AMHs are hominin groups that are morphologically and genetically distinct from each other. Modern humans evolved in Africa around 200,000 years ago, exited the continent about 60,000-50,000 years ago (or earlier), and reached Eurasia and Australia by about 50,000-45,000 years ago (see Groucutt et al., 2015 for a recent review). Regions adjacent to East Africa—Arabia, Sinai, the Levant, and the Iranian Plateau—record the first modern humans migrating out of this continent and, as 'first contact' areas, hold great palaeo-anthropological and archaeological potential. The weight of archaeological and fossil evidence suggests that Neanderthals evolved outside Africa, inhabiting Europe, western Asia, and the Middle East starting from, roughly, 250,000-300,000 years ago (see Hublin, 2009 for a review). Neanderthal occupation ended in Europe at around 41,000-39,000 (95.4% probability) calibrated (cal) years BP, strongly suggesting an overlap with AMHs for several thousand years in the region (Higham et al., 2014). Numerous hypotheses have attempted to explain the disappearance of Neanderthals from the archaeological record. These often involve the role of climate (e.g., Finlayson and Carrion, 2007; Jiménez-Espejo et al., 2007) and the perceived superiority of AMHs over Neanderthals in terms of technology, diet, and cognition (e.g., Binford, 1985; Mellars, 1989, Richards and Trinkaus, 2009). Recent ancient genetic research suggests that

Neanderthals and AMHs interbred outside of Africa (e.g., Green et al., 2010; Prüfer et al., 2014), resulting in the intrusion of Neanderthal-derived DNA at a proportion of 1.5-2.1% in all non-African modern humans (Prüfer et al., 2014).

### *2.2. The Zagros Mountains*

The Zagros Mountains are a series of parallel mountain ridges interspersed with plains that cross Iran from northwest to southeast, reaching the northeast of Iraq and the southeast of Turkey. The geomorphological setting of the Zagros, a karstic system reaching over 4,000 metres above sea level (m.a.s.l.), lends itself to the formation of caves that offer ample opportunities for both palaeoenvironmental and archaeological research. Given the physical geography of Iran, bounded in the north and south by mountains, the region has long been considered a potential dispersal corridor for hominins emerging out of Africa. Indeed, Vahdati Nasab et al. (2013) have posited a number of distinct migration routes according to the naturally occurring boundaries in the landscape, including a passageway through Iran, south of the Zagros Mountains.

### 2.3 *Previous research within the Zagros*

Early archaeological research in the Middle East began in the 1920s with researchers such as D.A.E. Garrod, who analysed local lithic assemblages in direct reference to European Palaeolithic traditions, i.e., the Mousterian (assigned to Neanderthals and the MP) and the Aurignacian (attributed to AMHs and the UP), according to their typological features (see Garrod, 1928, 1951; Garrod and Bate, 1942). In the 1950s, R. and R. Solecki excavated Shanidar Cave in Iraqi Kurdistan, where a number of Neanderthal individuals were found buried within the MP deposit (see Solecki, 1955, 1957, 1960, 1963; Solecki and Solecki, 1993). The UP material assemblage found at Shanidar Cave was considered to be sufficiently dissimilar to the Aurignacian to warrant a new, different name: 'Baradostian' (Solecki, 1957). In addition to this work, C.S. Coon excavated the sites of Bisitun, Tamtama and Khunik (Coon, 1951); R. Braidwood worked at Warwasi (Braidwood et al., 1961); F. Hole and K. Flannery excavated Kunji, Gar Arjeneh, Pa Sangar, Ghamari, and Yafteh Cave (Hole and Flannery, 1968); and M. Rosenberg investigated Eshkaft-e Gavi (Rosenberg 1985; Scott and Marean, 2009). In the early 1980s, field investigations in Iran decreased in frequency due to political instability and, as Vahdati Nasab (2011) suggests, the lack of enthusiasm shown by local archaeologists. During this time, workers re-evaluated archaeological collections stored outside of the Zagros. H.L. Dibble (1984), for instance, re-studied artefacts from Bisitun, and posited that, in contrast to

previous claims concerning the lack of Levallois[1] attributes in Mousterian industries from the Zagros, the assemblage showed a relatively high frequency of the technique. A decade later, through the re-analysis of the Warwasi assemblage, Olszewski and Dibble (1994) proposed the renaming of the Baradostian tradition to 'Zagros Aurignacian', given the perceived similarities with Aurignacian material, and suggested the possibility of an *in situ* origin for the Aurignacian industry. Beginning in the early 2000s and into the present, joint Iranian-European teams have surveyed, excavated, and reported results from multiple Palaeolithic sites across the Zagros Mountains (e.g., Conard et al., 2006; Jaubert et al., 2006; Otte et al., 2007; Conard and Ghasidian, 2011; Bazgir et al., 2014, 2017; Heydari-Guran and Ghasidian, 2017). This new field research may shed light on some of the major questions of interest to prehistorians in this region, including the issue of the origin of the Aurignacian and the Zagros Mountains, as well as the potential presence of mutually distinct and coeval lithic industries within the region during the UP (see Ghasidian et al., 2017).

### 3. Archaeological Sites

We have obtained new radiocarbon results for Kadar Cave, Ghār-e Boof, and Kobeh Cave, and analysed previously published chronometric data for the Zagros Mountain sites of Yafteh and Shanidar Cave (Figure 1). These archaeological sites are briefly described in the following sections.

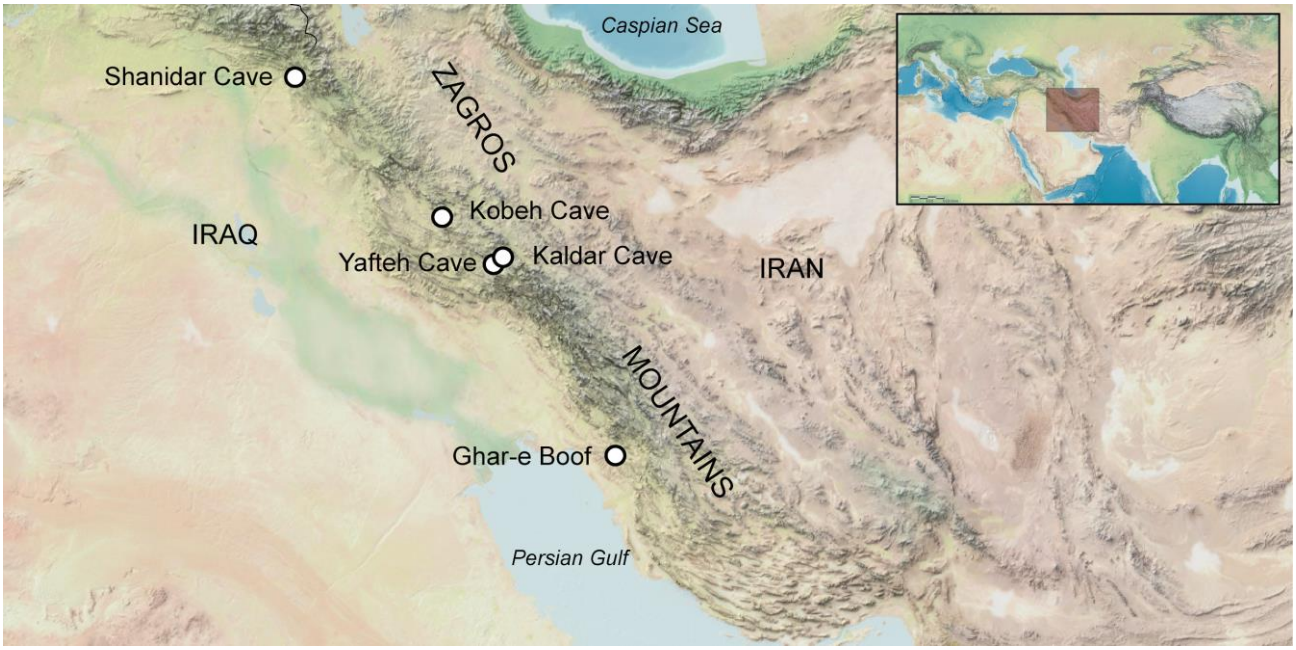


Figure 1. Location of archaeological sites investigated.

[1] The Levallois reduction technique for flake production is a representative element of the Mousterian industry (Bordes, 1961; Schlanger, 1996)

*3.1. Yafteh Cave*

Yafteh Cave is located in the Khorramabad region of Lorestan province, western Iran (at 1,278 m.a.s.l.; 33°30'30''N, 48°12'41''E), and was excavated in 1965 by Hole and Flannery (1968). The lithic technology at the site has assumed importance in discussions concerning the origin of the Aurignacian tradition due to its morphology and, as reported, similarity to European material (see Otte and Kozłowski, 2014). For this reason, a group from the University of Liège recommenced excavations at the site in 2005 and 2008. Following an analysis of the lithic assemblage, workers proposed an *in situ* development of the Aurignacian industry in the Zagros Mountains (Otte et al., 2007, 2011).

The stratigraphic sequence in Yafteh Cave contains 19 geological layers distinguished on the basis of soil colouration and texture (Figure 2). Bedrock was reached during the 2008 season at approximately 3 m in depth. Strata 1-4 correspond to historic and Islamic periods, while evidence for an UP tradition begins near the top of stratum 5 and continues until the bottom of the deposit.

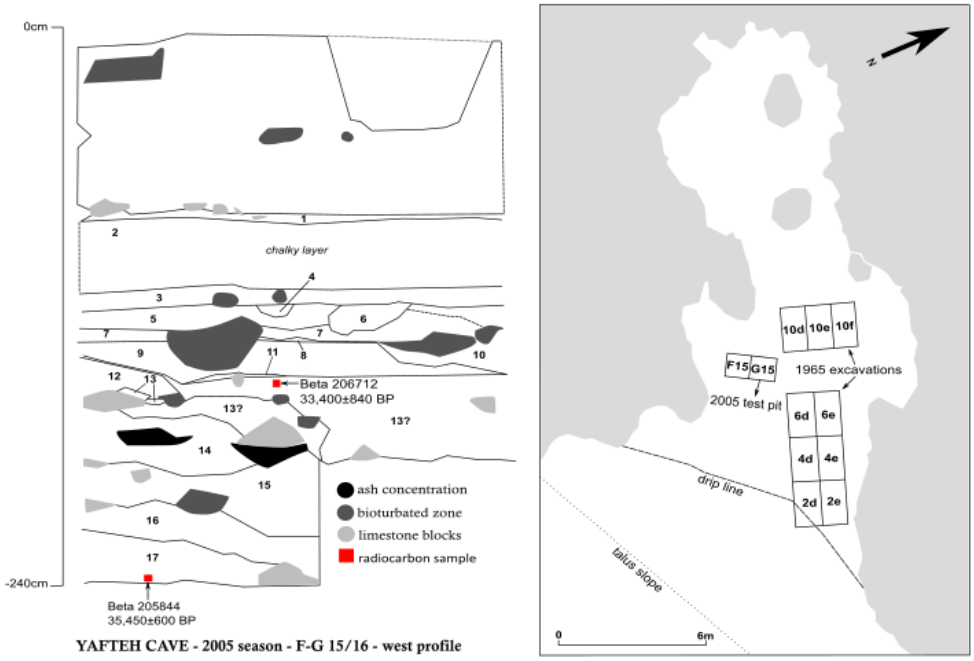


Figure 2. Schematic of the stratigraphy uncovered during the 2005 season (F-G 15/16, west profile) and floor plan at Yafteh Cave (modified from Otte et al., 2007).

In the 1960s, Hole and Flannery (1968) submitted a series of charcoal samples for radiocarbon dating. The sequence obtained showed age-depth incongruences and wide error margins. Additional charcoal samples were radiocarbon dated following the re-excavation of the site in the 2000s. Based on the new chronometric information, Otte et al. (2011) assigned a date of 33,400 ± 840 years BP (Beta-206712) to

the beginning of the UP sequence, and 35,450 ± 600 years BP (Beta-205844) to the bottom (Figure 2). All radiocarbon determinations were combined and ordered by Otte et al. (2011) according to depth (Table 1). There is little correspondence between early (1960s) and later (2000s) excavations as Hole and Flannery (1968) did not publish the exact location of their radiocarbon samples within the stratigraphy, and the material obtained by Otte et al. (2007) was collected from a different area within the cave.

Table 1. Published radiocarbon determinations for Yafteh Cave ordered by depth after Otte et al. (2011).

| Laboratory number | Collected (year) | Depth (below datum; cm) | Radiocarbon age (BP) |
|---|---|---|---|
| Beta-206711 | 2005 | 125 | 24,470 ± 280 |
| Beta-206712 | 2005 | 150 | 33,400 ± 840 |
| GX-711 | 1965 | 200 | 34,800 + 2900/-4500 |
| GX-710 | 1965 | 201 | 32,500 + 2400/-3400 |
| SI-332 | 1965 | 201 | 29,410 ± 1150 |
| Beta-245910 | 2008 | 210.5 | 33,800 ± 330 |
| SI-333 | 1965 | 212 | 30,860 ± 3000 |
| Beta-251058 | 2008 | 213 | 32,190 ± 290 |
| Beta-251062 | 2008 | 213.5 | 33,160 ± 240 |
| Beta-251059 | 2008 | 226.5 | 32,900 ± 290 |
| Beta-251060 | 2008 | 234 | 33,260 ± 300 |
| Beta-245908 | 2008 | 236 | 22,430 ± 310 |
| Beta-205844 | 2005 | 240 | 35,450 ± 600 |
| Beta-245909 | 2008 | 245 | 33,330 ± 310 |
| SI-336 | 1965 | 250 | 21,000 ± 800 |
| Beta-251061 | 2008 | 251 | 31,120 ± 240 |
| Beta-245913 | 2008 | 258.5 | 34,360 ± 340 |
| Beta-245907 | 2008 | 260 | 32,770 ± 290 |
| GX-709 | 1965 | 260 | 38,000 + 3400/-7500 |

| | | | |
|---|---|---|---|
| Beta-245911 | 2008 | 266.5 | 33,520 ± 330 |
| Beta-24912 | 2008 | 273 | 34,160 ± 360 |
| SI-334 | 1965 | 278 | 31,760 ± 3000 |
| GX-708 | 1965 | 280 | >36,000 |
| GX-707 | 1965 | 280 | 34,300 + 2100/-3500 |
| SI-335 | 1965 | 285 | >40,000 |
| GX-706 | 1965 | 290 | >35,600 |

*3.2. Shanidar Cave*

Shanidar Cave is situated on Baradost Mountain, Iraqi Kurdistan (44°13'E, 36°'50'N; Solecki, 1957, 1963). The cave is at 731.5 m.a.s.l. or 365.8 m above the Greater Zab River (Solecki, 1955). It has a length of 40 m, a maximum width of 53.34 m, and a total surface area of 1,200$m^2$ (Solecki, 1955, 1957, 1963). Shanidar Cave was originally excavated by R. Solecki from 1951 to 1960, in four separate seasons (years 1951, 1953, 1956-1957 and 1960; Solecki, 1955, 1957, 1960, 1963). After a long hiatus, excavations recommenced in recent years under G. Barker, University of Cambridge.

In 1951, R. Solecki began excavations with a sounding of 4.47 by 6.10m, reaching 7.62m in the deepest section. This was enlarged in 1953 to an area of 6.10 by 12.9 m, where bedrock was reached at a maximum depth of 13.41 m in the western portion of the sounding, and to 20 by 7.75 m in the 1957 season. Solecki divided the excavation area into 44 vertical levels (Solecki and Solecki, 1993) and identified four distinct archaeological layers—A, B, C, and D (Solecki, 1957). Layer A extends from modern times to the Neolithic, while Layer B contains no evidence of agriculture, animal domestication, or pottery making. Following Layer B, Solecki noted a gap in the stratigraphic sequence of a suggested span of 17,000 years, a period during which the cave was apparently left unoccupied. The sequence continues with Layer C, which marks an UP occupation. Layer D, sealed from the above deposit by rockfall within levels 14 and 15 (4.27-4.52 m from the surface), corresponds to the MP and a Neanderthal occupation (Solecki, 1957; Solecki and Solecki, 1993). Within this layer, the remains of 10 Neanderthal individuals were found (see Solecki, 1957, 1963, 1975; Trinkaus, 1978; Trinkaus and Zimmerman, 1982; Solecki and Solecki, 1993; Cowgill et al., 2007).

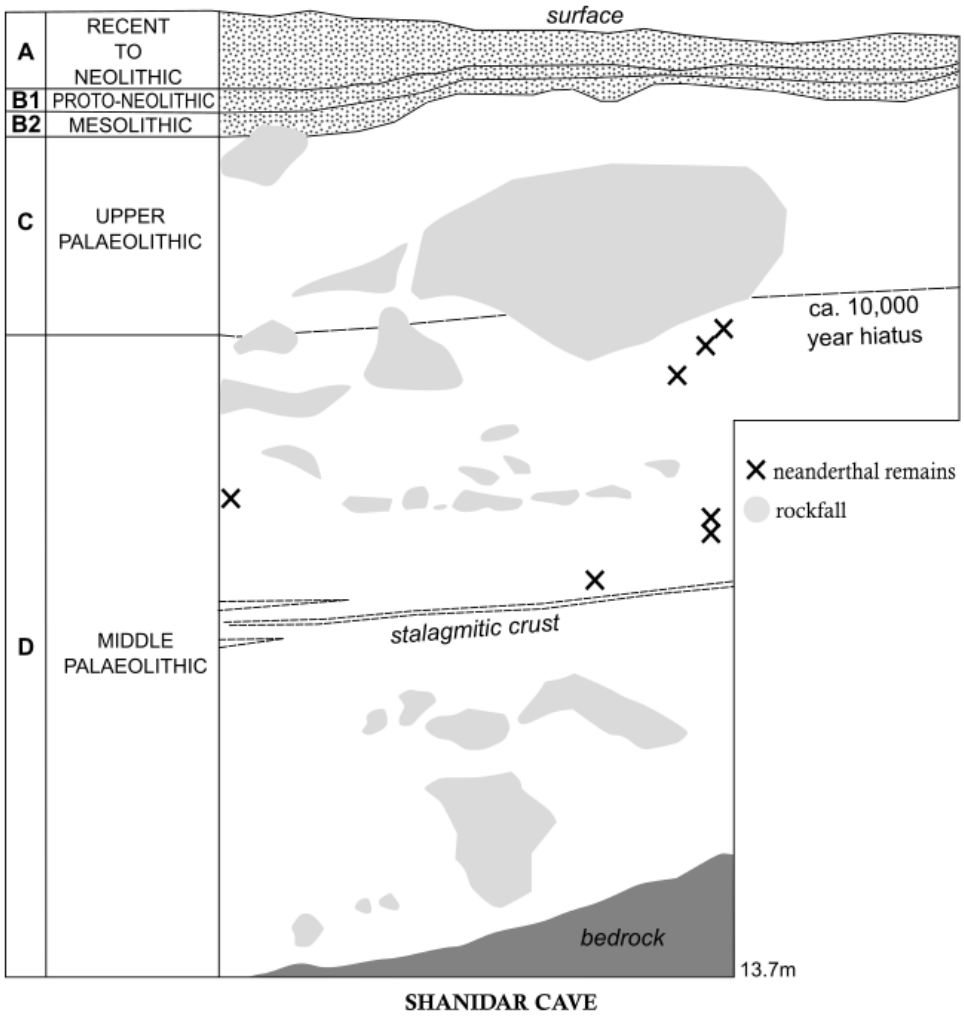


Figure 3. Schematic of the stratigraphy at Shanidar Cave (redrawn from Solecki, 1963).

The chronology of Shanidar Cave, in Solecki's time, was fixed by radiocarbon dates provided by four different laboratories (Table 2; Solecki, 1963). Apart from presenting some of these dates in publications, no further details concerning the materials or methods used in the dating process have been provided. Based on samples W-667 and W-179, Layer B1 was dated to 10,300 ± 300 years BP and B2 to 12,000 ± 400 years BP (Solecki, 1963). The top portion of Layer C was dated to 28,700 ± 700 years BP (sample W-654) and the bottom to 35,080 ± 500 years BP (GRO-259), while material taken from 5.1 m below the surface yielded a determination of 46,000 ± 1500 years BP (GRO-2527) for Layer D (Solecki, 1963). Additionally, several obsidian samples from Layers B and C were analysed using the obsidian hydration method (Evans and Meggers, 1960; Solecki, 1963). These determinations do not show a congruent age-depth pattern.

Table 2. Published radiocarbon determinations for Shanidar Cave. This list reflects available information from the published sources reviewed.

| Laboratory number | Archaeological Context | Date (BP) | Published source |
|---|---|---|---|
| W-667 | Layer B1 | 10600 ± 300 | Solecki, 1963 |
| W-179 | Layer B2 | 12000 ± 400 | Solecki, 1963 |
| W-654 | Layer C | 28700 ± 700 | Solecki, 1963; Hole and Flannery, 1968 |
| W-178 | Layer C (top); square S3W1; 3.05m deep | 29500 ± 1500 | Solecki, 1955; Hole and Flannery, 1968 |
| W-650 | Layer C | 33300 ± 1000 | Hole and Flannery, 1968 |
| GrN-1830 | Layer C | 33900 ± 900 | Hole and Flannery, 1968 |
| GrN-1494 | Layer C | 34400 ± 420 | Hole and Flannery, 1968 |
| GrN-2016 | Layer C | 35400 ± 600 | Hole and Flannery, 1968 |
| GrN-2015 | Layer C | 35540 ± 500 | Hole and Flannery, 1968 |
| GrN-2549 | Layer C | 35080 ± 500 | Solecki, 1963 |
| GrN-2527 | Layer D | 46900 ± 1500 | Solecki, 1963; Hole and Flannery, 1968 |
| GrN-1495 | Layer D | 50600 ± 3000 | Hole and Flannery, 1968 |

### *3.3. Kaldar Cave*

Kaldar Cave site is located in the Khorramabad Valley, Lorestan Province, western Iran (48°17’35’’E, 33°33’25’’N). The cave sits at 1,290 m.a.s.l., has a length of 16 m, a width of 17 m, and is 7 m high. An international team initially investigated Kaldar Cave during 2012, along with three other archaeological sites (Bazgir et al., 2014). This initial effort consisted of the opening of a 1 $m^2$ test pit at the very centre of the cave, which revealed a 1.5 m stratigraphic sequence containing multiple cultural levels. Following field observations, excavators realised that Kaldar Cave contained a better stratigraphic sequence than the other sites excavated. As such, a second excavation designed to obtain samples for dating and gain a better understanding of stratigraphic associations commenced in 2014. During this season, excavators opened a

3x3 m trench near the cave entrance and location of previous test pits (squares E5, E6, E7, F5, F6, F7, G5, G6 and G7) using 5 cm spits and recorded all findings within a three-dimensional (3D) grid. The trench exposed an approximately 2 m section of sedimentary deposit characterised by five main cultural layers (see Figure 4). Layers 1 to 3 (including sub-layers 4 and 4II) contain multiple phases dating to the Holocene; Layer 4 (including sub-layers 5, 5II, 6 and 6II), with its associated lithic technology, e.g., points, blades, and twisted bladelets, corresponds to the UP; and Layer 5 (including sub-layers 7 and 7II) contains a characteristic MP lithic assemblage with Levallois elements (Bazgir et al, 2014). So far, no chronometric data is available for Layer 5 (Bazgir et al., 2017).

### *3.4. Ghār-e Boof*

Ghār-e Boof, a small cave with a total surface area of 100 $m^2$, is situated in the Dasht-e Rostam region of Fars Province, southern Iran, at 905 m.a.s.l. (Conrad and Ghasidian, 2011). The site was excavated by the Tübingen Iranian Stone Age Research Project in 2006, 2007, and 2015. The predominant lithic component in the UP are bladelets belonging to a technocomplex termed 'Rostamian' by the excavators (Conard and Ghasidian, 2011; Ghasidian, 2014). A survey of 90 other caves and rockshelters of the Dasht-Rostam yielded Rostamian assemblages but, so far, excavations have only been conducted at Ghār-e Boof. The Rostamian tradition consists of a specialised mode of lithic reduction that is absent from contemporary sites along the Zagros Mountains, bearing no techno-typological resemblance to Aurignacian or Baradostian industries. As such, it is hypothesised that the Rostamian technocomplex evolved locally in the southern Zagros. This documents a high degree of cultural diversity in the region during the UP (Conard and Ghasidian, 2011; Ghasidian, 2014; Ghasidian et al., 2017).

During fieldwork, an area of 2 by 9m was excavated. This extended from the drip line to the back of the cave on a north-south axis. An elevation datum was assigned to the z-axis at an elevation of 8 m, and bedrock was reached at a depth of 5.5 m in the southern portion. Archaeological horizons (AH) were identified as such by material culture, soil colouration, and other distinctive features (Figure 6). At the top of the sequence, AH I and II correspond to Holocene silts and ash deposits. AH III corresponds to the UP as identified through a lithic assemblage composed of bladelets and bladelet cores. The stratigraphic sequence ends in unit 6/2 with Geological Horizon (GH) 4, containing AH IV, IVa, and IVb, also corresponding to the UP. The most recent excavation season, in 2015, reached MP deposits, but more fieldwork is required to obtain meaningful artefact assemblages from these basal layers.

Radiocarbon dating of two seed samples (OxA-25783 and OxA-25785) was previously undertaken at the Oxford Radiocarbon Accelerator Unit (ORAU), using a pre-treatment method designed to minimise the

destruction of material. These samples—legume remains found within AH IIIb at depths of 4.90 and 4.82 m, respectively—yielded dates of 33,850 ± 360 and 34,900 ± 650 years BP. Additional material was submitted for radiocarbon dating at the Leibnitz-Labor Laboratory, University of Kiel (Conard and Ghasidian 2011). Results obtained from two vetches (*Vicia ervilia*) from AH IV, the oldest stratum, were measured at 33,060 ± 270 BP and 36,030 ± 390 years BP.

### *3.5. Kobeh Cave*

Kobeh is a small cave (7x12 m) located near the capital of Kermanshah province, western Iran, in the west-central section of Zagros Mountains (47°10'8.25"E, 34°25'47.96"N; Marean and Kim, 1998). It is situated at an altitude of 1,300 m.a.s.l. near the Tang-i-Knisht Valley. Fieldwork led by B. Howe began at the site in 1959, with a 2x2.5 m test pit (Marean and Kim, 1998). From the surface, the entire excavated sequence extends to a depth of 3.2 m, where a rockfall event overlies a separate seemingly sterile horizon. Prior to a depth of 1.6 m, the presence of sporadic ceramic fragments and faunal remains is reported (Marean and Kim, 1998). Below this depth, layers P, Q, and R correspond to the terminal MP and include lithic and faunal material—the latter showing bone surface modification (Marean and Kim, 1998).

## 4. Materials and methods

Bone samples from Kobeh Cave (*n*=14) and Ghār-e Boof (*n*=42) were pre-screened for collagen preservation prior to sampling for radiocarbon dating (after Brock et al., 2010a). This step involved measuring the percent nitrogen (%N) in ~5 mg of whole bone powder (drilled and placed into a tin capsule) in a continuous flow isotope ratio mass spectrometer (Sercon 20/20), consisting of a CHN elemental analyser (Carlo-Erba NA, 2000) coupled to a gas source IRMS. Samples which show values lower than ~0.75 %N are not usually passed on to AMS radiocarbon dating, as they are not likely to contain sufficient collagen (<1% weight). All other materials—three seed samples from Ghār-e Boof, seven charcoal samples from Kaldar Cave, and one riverine snail from Ghār-e Boof—underwent the appropriate chemical pre-treatment method designed to remove exogenous carbon. These included the acid-base-wet oxidation/stepped combustion (ABOx-SC) protocol, phosphoric acid dissolution (see Brock et al., 2010b, for a detailed description of routine pre-treatment protocols used), and modified versions of ABOx-SC employed to avoid sample failure (Douka et al., in prep). ABOx-SC was chosen over the routine acid-base-acid (ABA) method, as it has been shown to remove contaminants more efficiently from Palaeolithic-aged charcoal samples, often yielding significantly older dates (e.g., Bird et al., 2003; Brock and Higham, 2009; Higham et al., 2009a, 2009b; Douka et al., 2010; Wood et al., 2012).

Following pre-treatment, dried samples were weighed and approximately 3-3.5 mg of material was combusted in the same CF-IRMS system employed for bone collagen pre-screening. Gaseous $CO_2$ produced during acid dissolution was inserted directly. After the measurement of carbon stable isotopes, the $CO_2$ was collected and transferred to pre-conditioned rigs containing a 2.0-2.5 mg iron catalyst and $H_2$ added at a ratio of $2.2H_2$:$CO_2$. These were heated at 560°C for six hours (Dee and Ramsey, 2000). Graphite targets were made with approximately 0.8 mg-1.8 mg of carbon, depending on the yield of each sample. Radiocarbon measurement was undertaken in a High Voltage Engineering Europa (HVEE) 2.5 MeV Accelerator Mass Spectrometer. Radiocarbon determinations were calculated according to the conventions outlined in Stuiver and Polach (1977).

The calibration and Bayesian modelling of radiocarbon determinations was undertaken using the OxCal 4.3 platform (Bronk Ramsey, 2009a, 2009b) and the IntCal13 calibration curve (Reimer et al., 2013). Radiocarbon dates in a Bayesian model are expressed in terms of a probability density function (PDF) through use of Markhov Chain Monte Carlo simulation approaches, which finds the highest probability distribution for these as weighed towards known archaeological information for each site. The statistical analysis is based on the assumption that a given chronological sequence is divided into separate units of time, called '`Phases`', which contain radiocarbon dates. `Phases` are constrained by '`boundaries`' which serve as mathematical functions and produce PDFs estimating the start and end of each `Phase`. By assigning each likelihood a prior probability of being an `outlier`, its influence on a given model is down-weighted, allowing for flexibility. As such, all dates modelled here were ascribed a 5% prior probability of being an `outlier` within the General t-type `Outlier Model` (Bronk Ramsey, 2009b).

## 5. Results

None of the faunal bone samples tested for %N reached the threshold of 0.75 (Table 3). These results suggested that no samples contained enough collagen for AMS radiocarbon dating, thus none was passed on for further pre-treatment.

Table 3. Pre-screening results (%N) of faunal bone samples from Kobeh Cave (KoC) and Ghār-e Boof (GB). Sample references followed by either 'A' or 'B' refer to sub-samples within the same bone fragment. The results suggest a uniformly low level of remaining collagen in the bones.

| Site | Sample reference | Combusted (wt; mg) | N (µg) | %N (wt) |
|---|---|---|---|---|
| KoC | 675 | 4.97 | 5.02949 | 0.101 |

| | | | | |
|---|---|---|---|---|
| KoC | 684 | 5.14 | 6.27834 | 0.122 |
| KoC | 690A | 4.99 | 5.37038 | 0.108 |
| KoC | 690B | 5.13 | 4.92662 | 0.096 |
| KoC | 702 | 4.95 | 4.69297 | 0.095 |
| KoC | 1988 | 5.06 | 6.00349 | 0.119 |
| KoC | 8096 | 5.7 | 8.04789 | 0.141 |
| KoC | 8217 | 4.97 | 5.84302 | 0.118 |
| KoC | 8642 | 5.08 | 6.00941 | 0.118 |
| KoC | 8968 | 5.08 | 15.11011 | 0.297 |
| KoC | 3672 | 5.11 | 3.69197 | 0.072 |
| KoC | 3680A | 5.07 | 17.27945 | 0.341 |
| KoC | 3680B | 4.93 | 13.16061 | 0.267 |
| KoC | 3695 | 4.9 | 7.55116 | 0.154 |
| KoC | 3818 | 4.81 | 4.92294 | 0.102 |
| KoC | 3827 | 4.8 | 5.90319 | 0.123 |
| GB | 1A | 2.61 | 5.59388 | 0.21 |
| GB | 1B | 2.79 | 5.99152 | 0.21 |
| GB | 2A | 2.46 | 5.05467 | 0.21 |
| GB | 2B | 2.48 | 5.36492 | 0.22 |
| GB | 3A | 2.73 | 4.61503 | 0.17 |
| GB | 3B | 2.58 | 3.67806 | 0.14 |
| GB | 4A | 2.5 | 6.13677 | 0.25 |
| GB | 4B | 2.67 | 7.37776 | 0.28 |
| GB | 5A | 2.99 | 5.58735 | 0.19 |
| GB | 5B | 2.84 | 5.69284 | 0.2 |
| GB | 6A | 3 | 6.07218 | 0.2 |

| | | | | |
|---|---|---|---|---|
| GB | 6B | 2.78 | 7.05446 | 0.25 |
| GB | 7A | 2.35 | 4.9019 | 0.21 |
| GB | 7B | 2.46 | 5.50677 | 0.22 |
| GB | 8 | 2.79 | 7.28358 | 0.26 |
| GB | 9 | 2.93 | 5.30434 | 0.18 |
| GB | 10A | 2.82 | 6.60423 | 0.23 |
| GB | 10B | 2.8 | 6.23539 | 0.22 |
| GB | 11A | 2.69 | 8.31874 | 0.31 |
| GB | 11B | 2.76 | 7.28077 | 0.26 |
| GB | 12A | 3.03 | 7.33149 | 0.24 |
| GB | 12B | 2.45 | 3.35461 | 0.14 |
| GB | 13 | 2.28 | 5.73843 | 0.25 |
| GB | 14 | 2.82 | 5.1007 | 0.18 |
| GB | 15 | 2.98 | 5.79644 | 0.19 |
| GB | 16 | 2.8 | 3.96831 | 0.14 |
| GB | 17 | 2.71 | 7.74739 | 0.29 |
| GB | 18 | 2.78 | 6.59087 | 0.24 |
| GB | 19 | 2.38 | 6.11892 | 0.26 |
| GB | 20 | 3.22 | 5.60614 | 0.17 |
| GB | 21 | 2.94 | 5.1426 | 0.17 |
| GB | 22 | 2.67 | 5.21032 | 0.2 |
| GB | 23 | 2.98 | 7.22746 | 0.24 |
| GB | 24 | 3.17 | 7.2795 | 0.23 |
| GB | 25 | 2.72 | 4.82615 | 0.18 |
| GB | 26 | 2.96 | 6.71204 | 0.23 |
| GB | 27 | 2.26 | 3.94588 | 0.17 |

| | | | | |
|---|---|---|---|---|
| GB | 28 | 2.5 | 5.27486 | 0.21 |
| GB | 29 | 2.99 | 5.20558 | 0.17 |
| GB | 30 | 2.36 | 4.57249 | 0.19 |
| GB | 31 | 3.2 | 2.65732 | 0.08 |
| GB | 32 | 2.71 | 6.20176 | 0.23 |
| GB | 33 | 2.63 | 3.19625 | 0.12 |
| GB | 34 | 3.14 | 4.09168 | 0.13 |
| GB | 35 | 2.96 | 4.26613 | 0.14 |
| GB | 36 | 3.19 | 4.00298 | 0.13 |
| GB | 37 | 3.22 | 5.21662 | 0.16 |
| GB | 38 | 2.91 | 3.52456 | 0.12 |
| GB | 39 | 2.97 | 4.72232 | 0.16 |
| GB | 40 | 3.2 | 3.30962 | 0.1 |
| GB | 41 | 2.72 | 5.75578 | 0.21 |
| GB | 42A | 3.17 | 2.26344 | 0.07 |
| GB | 42B | 2.59 | 1.5701 | 0.06 |

Of seven charcoal samples processed, only five from Kaldar Cave passed chemical pre-treatment and were AMS dated (Tables 4, 5; these results are also noted in Bazgir et al., 2017). Of these, two yielded modern dates incongruent with their position in the stratigraphy. This is likely because the two charcoal samples were general finds and their exact location within the stratigraphy is not known (see Table 4; Figure 4). Considering that only three reliable dates were obtained for Kaldar Cave, no modelling was undertaken. From Ghār-e Boof, two out of four samples analysed (three seeds and one riverine snail) passed pre-treatment and were AMS dated (Tables 4, 5; Figure 6). The snail sample (OxA-32390), collected from AH IV, yielded a comparatively younger date than the seed taken from AH III (OxA-X-2633-54) and was duly identified as an outlier in the model created (at 91% probability; Figure 5). This age-depth discrepancy has a number of potential explanations. The two most parsimonious are i. post-depositional mixing within the sequence, e.g., bioturbation, or ii. modern carbon contamination resulting in an underestimation of the true

age. The first explanation cannot be ruled out. The second applies to the carbonate if the presence of recrystallized calcite is detected or other sources of modern carbon are somehow introduced during laboratory procedures. In this case, both are unlikely as the snail shell was tested using geological staining techniques (Friedman, 1959) prior to acid dissolution and found to be aragonitic, while the procedural blank that accompanied it during dating procedures showed no significant levels of modern carbon contamination (fM = 0.00001 ± 0.00023). There is a chance, however, that the pre-treatment protocol used for the seed was not rigorous enough to remove modern carbon contamination. A modified version of ABOx-SC which omitted a base wash and stepped combustion was utilised in this particular case, as organics often completely disintegrate during the strong base (1 M NaOH) rinse and carbonised seeds, or samples of small mass, fail at the last oxidation stage. Due to the small size of the seed sample processed (11.05 mg), the experimental protocol used in the dating of this sample focused on retaining enough material post treatment for dating. Considering this, it is suggested that further dating efforts for Ghār-e Boof and other archaeological sites in the region focus primarily on single entity organics which have a weight appropriate for the most rigorous pre-treatment methods. For old charcoal, a starting weight of ~100 mg or more is recommended for the ABOx-SC protocol, or ~50mg for the new modified protocol (Douka et al. in prep).

The Bayesian model created for this site incorporates previously published radiocarbon determinations (Conard and Ghasidian, 2011) and the two AMS dates obtained, yielding a start `boundary` for the UP at 41,900-40,050 cal BP (68.1% probability; Fig. 5). The model identified two `outliers` (Find 209.1 and OxA-32390) and resulted in bimodal distributions, especially for the end of AH III**.**

Table 4. Details of samples from Kaldar Cave (KaC) and Ghār-e Boof (GB) which passed chemical pre-treatment and were AMS radiocarbon dated.

| Site | Sample reference | Material | Species | Archaeological context |
|---|---|---|---|---|
| KaC | 723 | charcoal | *Prunus* cf. *amygdalus* | Trench (T) 1; Level 4, sub-level 5; SQ E6; 69 (X), 12 (Y), 110 (Z) |
| KaC | non-provided; 'A' | charcoal | *Quercus* sp. deciduous | T1; Level 4, sub-level 5; SQ G6 |
| KaC | non-provided; 'B' | charcoal | *Quercus* sp. deciduous | T1; Level 5, sub-level 7II; SQ F7 |

| | | | | |
|---|---|---|---|---|
| KaC | 274 | charcoal | *Prunus* cf. *amygdalus* | T 1; Level 4, sub- level 5; SQ E7; 78 (X), 5 (Y), 85 (Z) |
| KaC | 869 | charcoal | *Prunus* cf. *amygdalus* | T1; Level 4, sub-level 5II; SQ E6; 45 (X), 100 (Y), 125 (Z) |
| GB | find no. 206 | seed | *Lathyrus* sp. | AH III; GH 3; unit 6/2; 587 (Z) |
| GB | find no. 236 | snail | *Theodoxus* sp. | AH IV; GH 4; unit 6/2; 565 (Z) |

Table 5. AMS radiocarbon dates for the sites of Kaldar Cave (KaC) and Ghār-e Boof (GB).

| Site | Sample reference | ORAU Lab code | $\delta^{13}C$ (‰) | Radiocarbon date (BP) | Calibrated date (95.4% probability) |
|---|---|---|---|---|---|
| KaC | 723 | OxA-32238 | -23 | 33,480 ± 320 | 38650-36750 cal BP |
| KaC | 'A' | OxA-32239 | -23.1 | 964 ± 26 | 1000-1200 AD |
| KaC | 'B' | OxA-32240 | -27.1 | 1.09665 ± 0.00323 | 1850-1950 AD |
| KaC | 274 | OxA-X-2645-11 | -23.4 | 39,300 ± 550 | 44200-42350 cal BP |
| KaC | 869 | OxA-X-2645-12 | -24.5 | 49,200 ± 1800 | 54400-46050 cal BP |
| GB | find no. 206 | OxA-X-2633-54 | -21.3 | 35950 ± 800 | 42050-38950 cal BP |
| GB | find no. 236 | OxA-32390 | -6.7 | 31620 ± 180 | 36000-35000 cal BP |

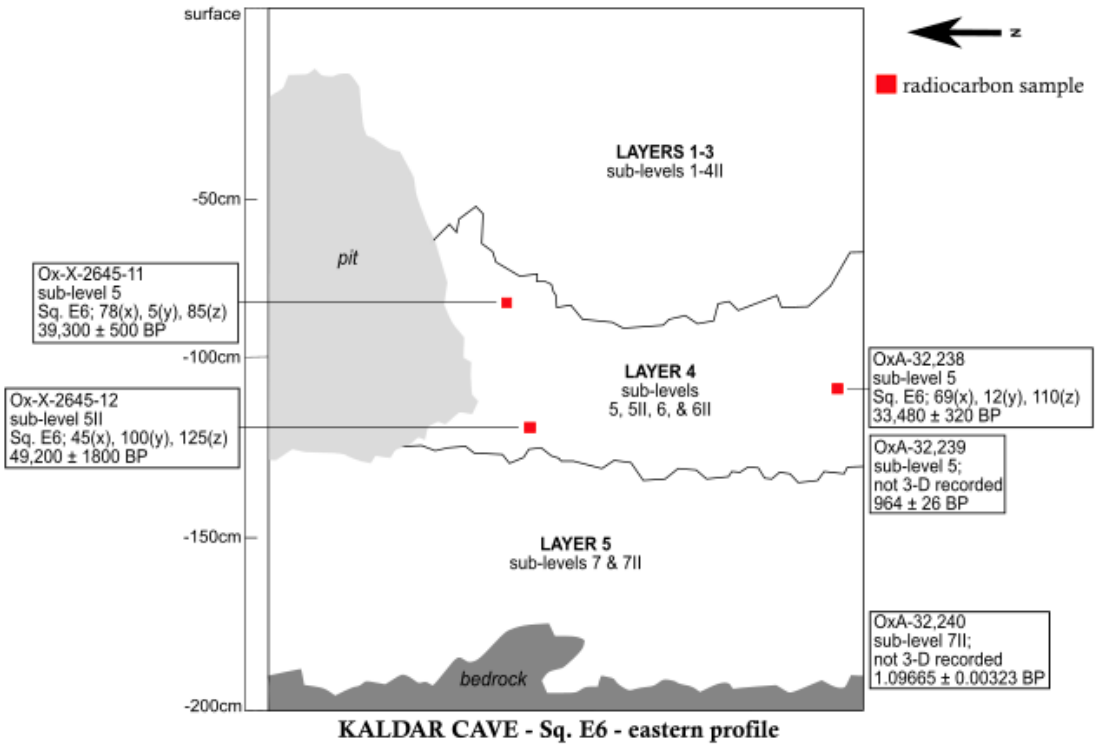


Figure 4. Schematic of the stratigraphic sequence at Kaldar Cave (SQ E6, eastern profile), showing the location of samples that were AMS radiocarbon dated.

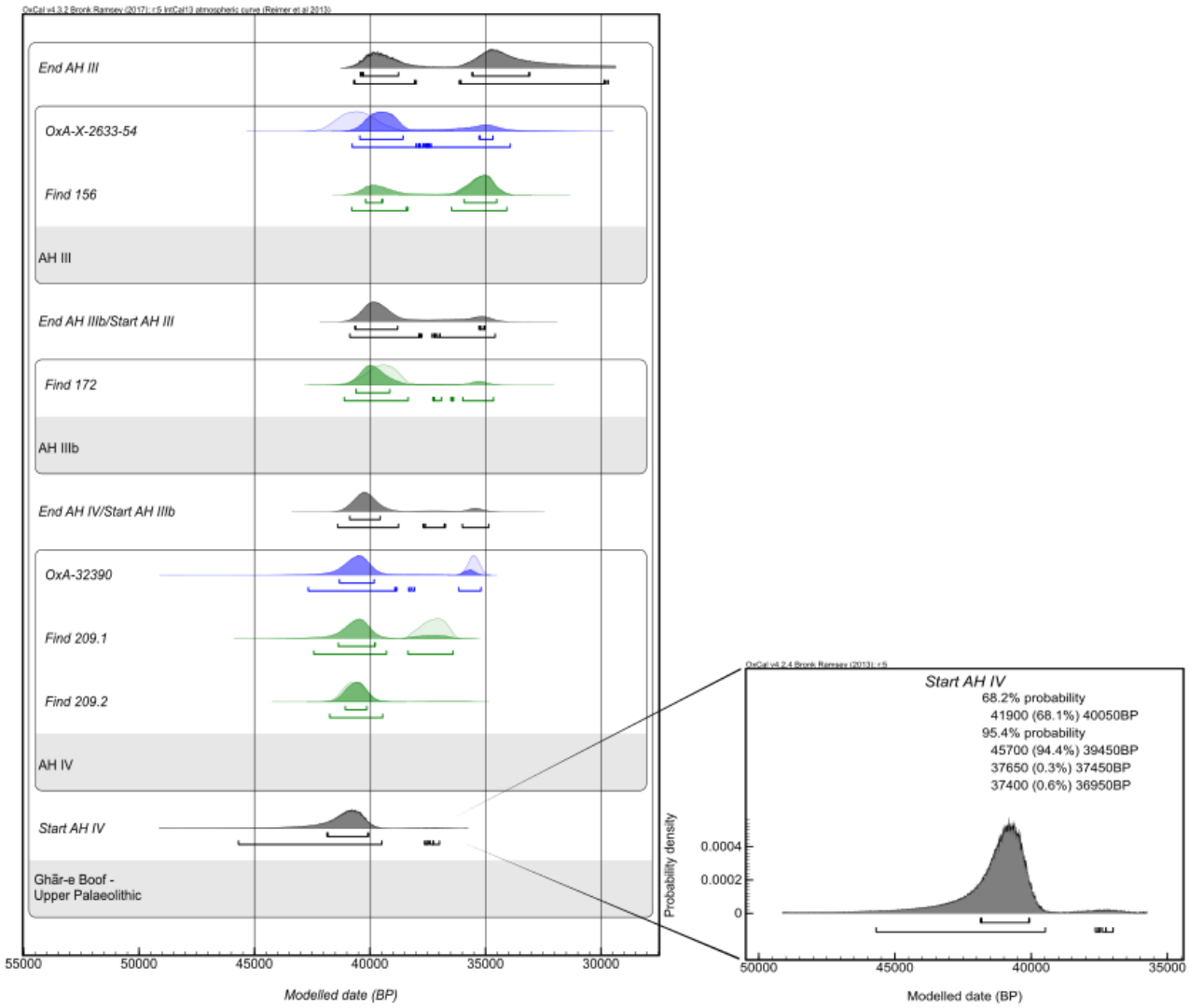


Figure 5. Bayesian model of radiocarbon dates for the Upper Palaeolithic sequence at Ghār-e Boof, including those published by Conard and Ghasidian (2011; in green), and the two OxA dates obtained (in blue). This model has three separate phases corresponding to AHs IV, IIIb, and III. OxCal CQL code is provided in Supplementary Online Material (SOM).

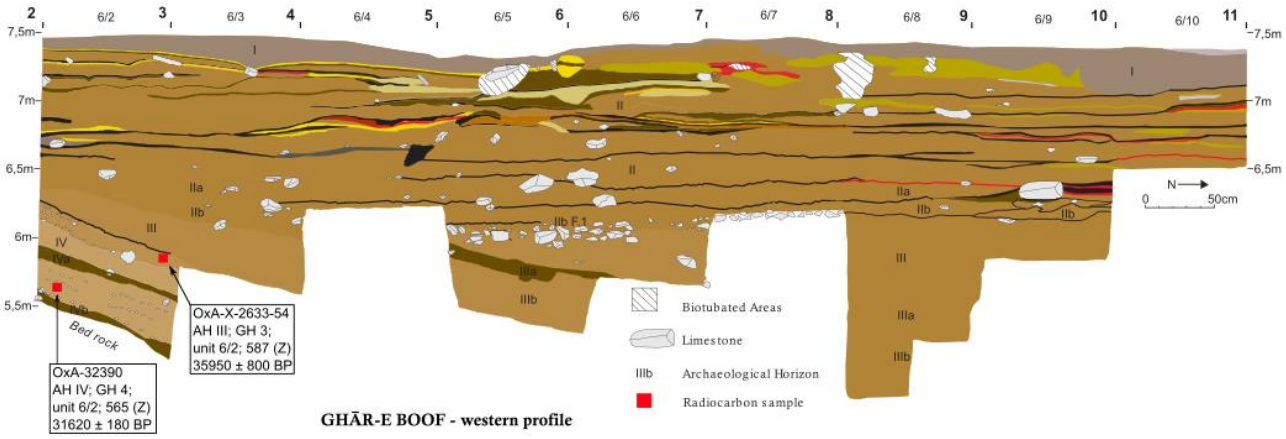

Figure 6. Schematic of the stratigraphic sequence at Ghār-e Boof (western profile), showing the location of AMS radiocarbon dated samples. After Conard and Ghasidian, 2011, Figure 7.

For Yafteh Cave, a Bayesian model incorporating radiocarbon determinations published by Otte et al. (2011) and their respective depths in a sequence yields a date `boundary` for the beginning of the UP at 38,850-38,000 cal BP (68.3% probability; Fig. 7). Beta-251061, Beta-205844, and Beta-206711 are identified as `outliers` at likelihoods of 100%, 90%, and 100%, respectively. The radiocarbon determinations obtained by Hole and Flannery (1968) were not included in this model as they show wide error margins and, as discussed, their stratigraphic relationship with the samples obtained in the 2000s is unknown.

For Shanidar cave, modelling the radiocarbon determinations obtained in the 1960s (Solecki, 1963; Hole and Flannery, 1968) for Layers B1, B2, C, and D, results in a PDF for the start `boundary` of the UP at 43,200-39,600 cal BP (68.2% probability) with no `outliers` (Figure 8).

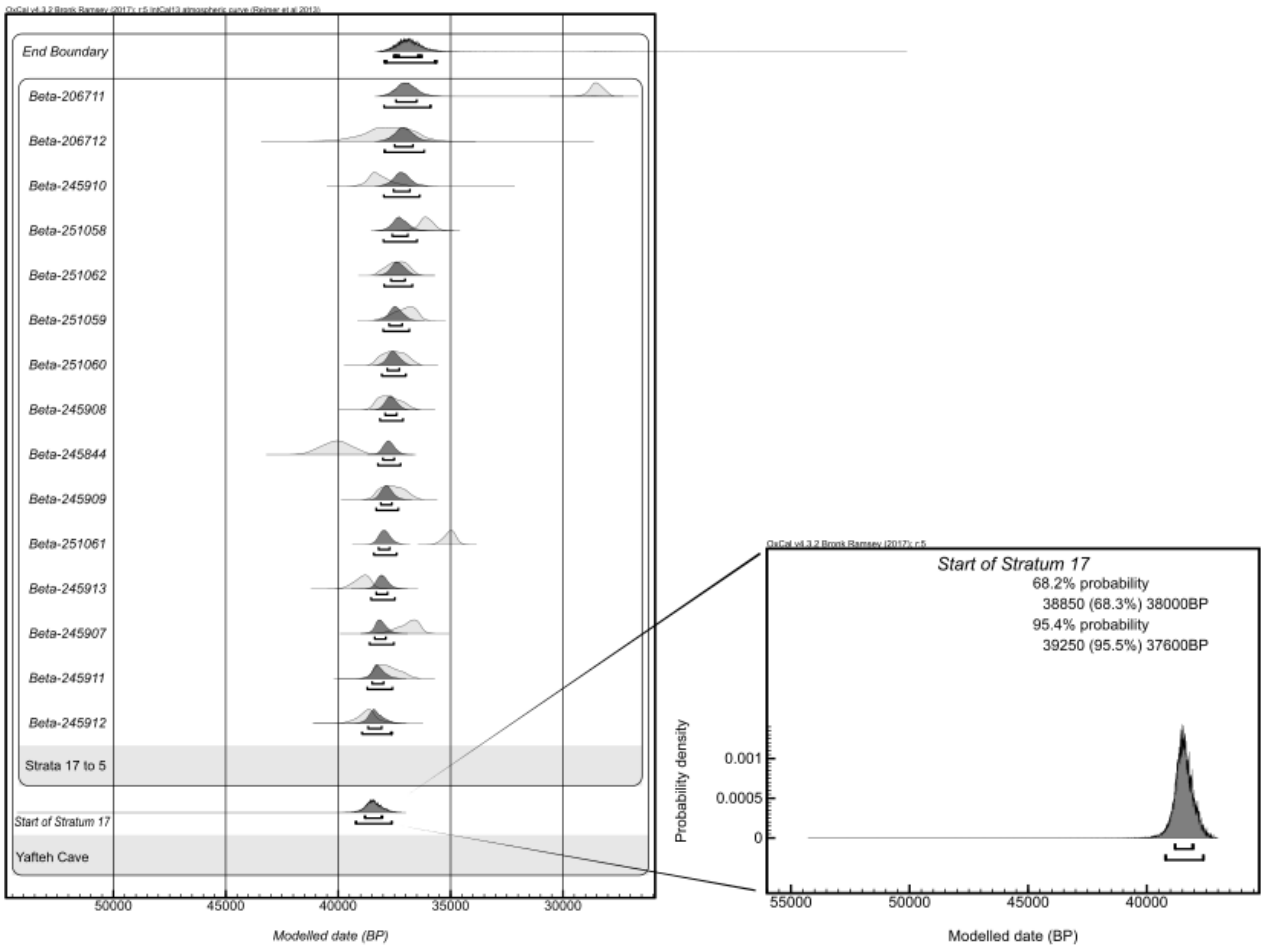


Figure 7. Bayesian model of radiocarbon dates for the Upper Palaeolithic sequence at Yafteh Cave, including those obtained in the 2000s as published by Otte et al. (2011:3). OxCal CQL code in SOM.

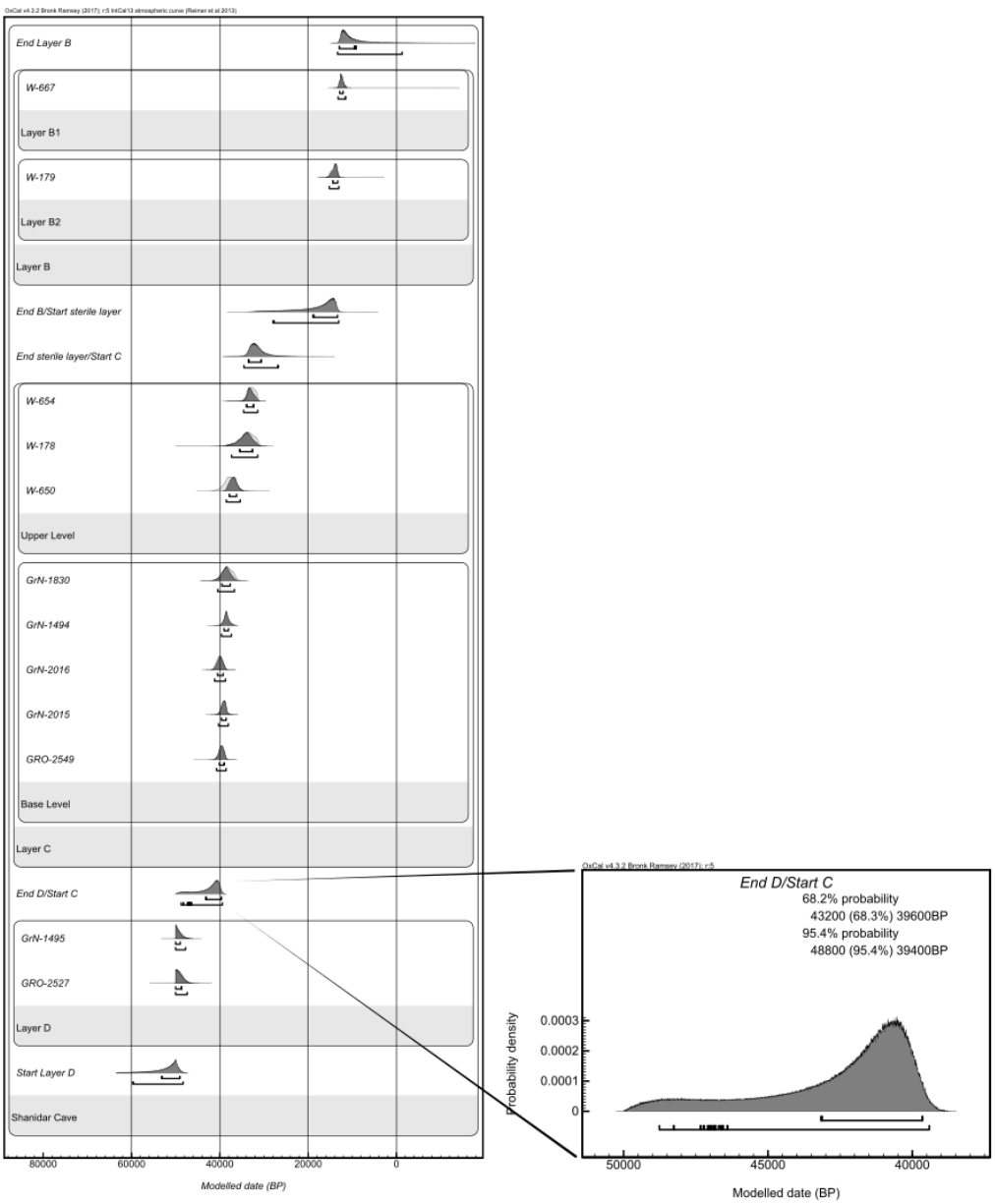


Figure 8. Bayesian model of radiocarbon dates for Layers D, C, and B at Shanidar Cave, as published by Hole and Flannery (1968), and Solecki (1963). OxCal CQL code is shown in the SOM.

The incorporation of PDFs generated for the end of the MP/start of the UP for Yafteh Cave, Ghār-e Boof, and Shanidar Cave into a single Bayesian model, results in a start `boundary` for the M-UP transition at the Zagros Mountains dating to 45,100-40,350 (68.2% probability) cal BP (Figure 9).

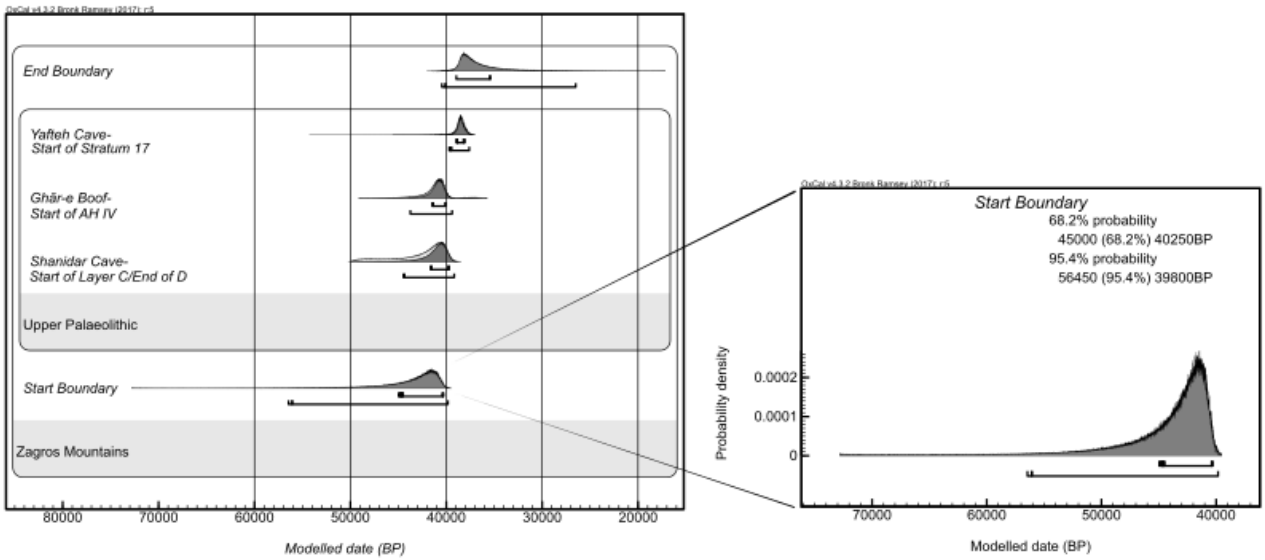


Figure 9. Bayesian model for the Middle to Upper Palaeolithic transition in the Zagros Mountains, using modelled chronometric data for Yafteh Cave, Ghār-e Boof, and Shanidar Cave.

## 6. Discussion

Based on the small number of new determinations which we were able to obtain, it is clear that further work is required if we are to achieve robust site chronologies and increase the temporal resolution of the M-UP transition in the Zagros Mountains. We encountered severe difficulties with the radiocarbon dating of bone from the region, and our pre-screening efforts showed that bones containing collagen are rare. Collagen is affected by the combined influences of post-depositional temperature, moisture content, bacterial presence and site pH, which together cause the loss of collagen through diagenetic processes (see Collins et al., 2002; Hedges, 2002). Under certain circumstances, this reduces the number of bones from a given site which are suitable for dating, restricting the potential to reliably date an archaeological sequence. Attempting to date material from archaeological sites known to yield poorly preserved bones with low collagen content is, therefore, an inefficient use of time and resources. Unfortunately, %N results for Kobeh Cave and Ghār-e Boof suggest that this might very well be the case for the Zagros Mountains—no pre-screened samples passed 0.4 %N, showing that collagen preservation was exceptionally poor. The data is not without value, however, as it does suggest that chronometric investigations in the region ought to focus on other types of organic material. The radiocarbon dating of charcoal, for example, will most likely produce a higher number of AMS radiocarbon dates. It is important to emphasise, however, that in the dating of Palaeolithic-aged charcoal, rigorous pre-treatment methods should be employed in order to obtain robust results. The routinely used ABA protocol has been shown to consistently underestimate the age of ‘old’ charcoal when compared

to ABOx-SC. The younger date range obtained for the UP start boundary at Yafteh Cave, in comparison to the other sites investigated, is likely to be an underestimate based on the use of ABA techniques in the preparation of previously obtained dates. If additional material were secured in the future, the use of more rigorous pre-treatment protocols would likely provide a more reliable, probably older, chronology for the site.

It is important that we continue our efforts to improve the chronology of Zagros sites due to the archaeological importance of the region and the likely elucidation of spatio-temporal dynamics in hominin dispersal through this process. Future chronometric investigations focused on terminal MP sequences within the region, for instance, will help to determine the nature of the transition and whether it involved a direct replacement of Neanderthals by modern humans or not. Therein lies the importance of archaeological and chronometric research in sites like Kaldar and Shanidar Cave, which contain both Middle and Upper Palaeolithic sequences.

## 7. Conclusion

High-precision AMS radiocarbon dates were obtained for the Upper Palaeolithic layers of Kaldar Cave and Ghār-e Boof—key archaeological sites within the Zagros Mountains. These, along with the statistical analysis of previously published radiocarbon determinations for the sites of Yafteh Cave (Iran) and Shanidar Cave (Iraqi Kurdistan), allowed us to build preliminary age models using Bayesian modelling with OxCal 4.3. The date boundary obtained for the start of the UP in the Zagros Mountains (40,000-45,250 cal BP at 68.2% confidence) is similar to estimates for the start of the UP in other parts of Eurasia, including the Levant (e.g., Douka, 2013) and Europe (e.g., Wood et al., 2014), but does not significantly predate them. Pre-screening efforts focused on faunal bone remains demonstrated that for Kobeh Cave and Ghār-e Boof, collagen preservation is low and yields are insufficient for radiocarbon dating. These results suggest that chronometric efforts for the Zagros region might do best to focus on dating other organic remains, such as charcoal, using rigorous pre-treatment methods which sufficiently decontaminate Palaeolithic-aged material. Our preliminary results and Bayesian models provide a starting point for further work in developing higher precision data of relevance for understanding the Middle to Upper Palaeolithic transition in this key region for hominin dispersal.

## Acknowledgments

The research leading to these results has received funding from the European Research Council under the European Union's Seventh Framework Programme (FP7/2007-2013); ERC grant 324139 “PalaeoChron” awarded to Professor Tom Higham. We thank all members of the project; the staff of the Oxford Radiocarbon

Accelerator Unit, University of Oxford; and Mariana Sontag González for her review of the manuscript. Work at Kaldar Cave was supported by the MINECO-FEDER (project CGL2015-65387-C3-1-P), AGAUR (project SGR 2014-899), and the URV (projects 2014/2015/2016PFR-URV-B2-17). B. Bazgir is a beneficiary of the Fundación Atapuerca pre-doctoral grant. L. Tumung holds a IDQP pre-doctoral scholarship at URV. Research at IPHES is framed under the CERCA Programme/Generalitat de Catalunya. Investigations at Khorramabad region are part of an agreement between IPHES and RICHT, supported by ICAR. We are especially thankful to both directors (Seyed Mohammad Beheshti and Hamide Chubak).

**References**

Ash P.J., Robinson D.J., 2011. The Emergence of Humans: An Exploration of the Evolutionary Timeline. John Wiley & Sons, West Sussex.

Bar-Yosef O., 2002. The upper paleolithic revolution. A. Rev. Anthropol. 31, 363-393.

Bazgir, B., Otte, M., Tumung, L., Ollé, A., Deo, S.G., Joglekar, P., López-García, J.M., Picin, A., Davoudi, D., van der Made, J., 2014. Test excavations and initial results at the Middle and Upper Paleolithic sites of Gilvaran, Kaldar, Ghamari caves and Gar Arjene Rockshelter, Khorramabad Valley, western Iran. C. R. Palevol. 13, 511-525.

Bazgir, B., Ollé, A., Tumung, L., Becerra-Valdivia, L., Douka, K., Higham, T., van der Made, J., Picin, A., Saladié, P., López-Garcí-a, J.M., Blain, H.-Al., Allué, E., Fernández-García, M., Rey-Rodríguez, I., Arceredillo, D., Bahrololoumi, F., Azimi, M., Otte, M.,. Carbonell, E., 2017. Understanding the emergence of modern humans and the disappearance of Neanderthals: Insights from Kaldar Cave (Khorramabad Valley, Western Iran). Sci. Rep. 7, 43460.

Binford L.R., 1985. Human ancestors: Changing views of their behavior. J. Anthropol. Archaeol. 4, 292-327.

Bird, M.I., Fifield, L.K., Santos, G.M., Beaumont, P.B., Zhou, Y., Di Tada, M.L., Hausladen, P.A., 2003. Radiocarbon dating from 40 to 60ka BP at Border Cave, South Africa. Quaternary Sci. Rev. 22, 943-947.

Bordes F., 1961. Mousterian cultures in France: Artifacts from recent excavation dispel some popular misconceptions about Neanderthal man. Science 134, 803-810.

Braidwood R.J., Howe B., Reed C.A., 1961. The Iranian prehistoric project: New problems arise as more is learned of the first attempts at food production and settled village life. Science 133, 2008-2010.

Brock F., Higham T., 2009. AMS radiocarbon dating of paleolithic-aged charcoal from Europe and the Mediterranean rim using ABOx-SC. Radiocarbon 51, 839-846.

Brock F., Higham T., Ramsey C.B., 2010a. Pre-screening techniques for identification of samples suitable for radiocarbon dating of poorly preserved bones. J. Archaeol. Sci. 37, 855-865.

Brock F., Higham T., Ditchfield P., Bronk Ramsey C., 2010b. Current pretreatment methods for AMS radiocarbon dating at the Oxford Radiocarbon Accelerator Unit (ORAU). Radiocarbon 52, 103-112.

Bronk Ramsey C.B., 2009a. Bayesian analysis of radiocarbon dates. Radiocarbon 51, 337-360.

Bronk Ramsey C.B., 2009b. Dealing with outliers and offsets in radiocarbon dating. Radiocarbon 51, 1023-1045.

Collins, M.J., Nielsen–Marsh, C.M., Hiller, J., Smith, C.I., Roberts, J.P., Prigodich, R.V., Wess, T.J., Csapo, J., Millard, A.R., Turner–Walker, G., 2002. The survival of organic matter in bone: A review. Archaeometry 44, 383-394.

Conard N., Ghasidian E., 2011. The Rostamian cultural group and the taxonomy of the Iranian Upper Paleolithic. In: Conard N., Drechsler P., Morales A. (Eds.), Between Sand and Sea: the Archaeology and Human Ecology of Southwestern Asia. Kerns Verlag, Tübingen, pp. 33-52.

Conard N.J., Ghasidian E., Heydari S., Zeidee M., 2006. Report on the 2005 survey of the Tübingen-Iranian Stone Age research project in the provinces of Esfahan, Fars and Kohgiluyeh-Boyerahmad. Archaeol. Rep. 5, 9-34.

Coon, C.S., 1951. Cave Explorations in Iran, 1949. Museum Monographs, The University of Pennsylvania, Philadelphia.

Cowgill L.W., Trinkaus E., Zeder M.A., 2007. Shanidar 10: A middle Paleolithic immature distal lower limb from Shanidar cave, Iraqi Kurdistan. J. Hum. Evol. 53, 213-223.

Dee M., Ramsey C.B., 2000. Refinement of graphite target production at ORAU. Nucl. Instr. Meth. Phys. Res. B. 172, 449-453.

Dibble H.L., 1984. The Mousterian industry from Bisitun cave (Iran). Paléorient 10, 23-34.

Douka, K. 2013. Exploring “the great wilderness of prehistory”: The chronology of the Middle to the Upper Palaeolithic transition in the northern Levant. Mitteilungen der Gesellschaft für Urgeschichte 22, 11–40.

Douka K., Higham T., Sinitsyn A., 2010. The influence of pretreatment chemistry on the radiocarbon dating of Campanian Ignimbrite-aged charcoal from Kostenki 14 (Russia). Quatern. Res. 73, 583-587.

Douka, K., Comeskey, D., Becerra Valdivia, L., McBeath, A., Ascough, P., Bird, M., Higham, T. An improved new methodology (AOx-SC) for the reliable radiocarbon dating of old charcoal (in preparation).

Evans C., Meggers B.J., 1960. Part II, An archaeological evaluation of the method. Am. Antiq. 25, 523-537.

Finlayson C., Carrion J.S., 2007. Rapid ecological turnover and its impact on Neanderthal and other human populations. Trends Ecol. Evol. 22, 213-222.

Friedman G.M., 1959. Identification of carbonate minerals by staining methods. J. Sediment. Res. 29, 87-97.

Garrod, D.A., 1928. Excavation of a Palaeolithic cave in Western Judaea. Palestine Exploration Quarterly. 60, 182-185.

Garrod, D.A., Bate, D.M., 1942. Excavations at the Cave of Shukbah, Palestine, 1928. Proc. Prehis. Soc. 8, 1-20.

Garrod, D.A.E. 1951. A transitional industry from the base of the Upper Palaeolithic in Palestine and Syria. J. Roy. Anthropol. Inst. of Great Britain and Ireland. 81, 121–130.

Ghasidian E., 2014. The Early Upper Paleolithic Occupation at Ghār-e Boof Cave: A Reconstruction of Cultural Tradition in the Southern Zagros Mountains of Iran. Kerns, Tübingen.

Ghasidian, E., Bretzke, K., Conard, N.J., 2017. Excavations at Ghār-e Boof in the Fars Province of Iran and its bearing on models for the evolution of the Upper Palaeolithic in the Zagros Mountains. J. Anthropol. Archaeol. 47, 33-49.

Green, R.E., Krause, J., Briggs, A.W., Maricic, T., Stenzel, U., Kircher, M., Patterson, N., Li, H., Zhai, W., Fritz, M.H.Y., Hansen, N.F., 2010. A draft sequence of the Neandertal genome Science. 328, 710-722.

Groucutt, H.S., Petraglia, M.D., Bailey, G., Scerri, E.M., Parton, A., Clark-Balzan, L., Jennings, R.P., Lewis, L., Blinkhorn, J., Drake, N.A., Breeze, P.S., Inglis, R.H., Devès, M.H., Meredith-Williams, M., Boivin, N., Thomas, M.G., Scally, A., 2015. Rethinking the dispersal of *Homo sapiens* out of Africa. Evol. Anthr. 24,149-164.

Hedges R.E., 2002. Bone diagenesis: An overview of processes. Archaeometry 44, 319-328.

Heydari-Guran, S., Ghasidian, E., 2017. The MUP Zagros Project: tracking the Middle–Upper Palaeolithic transition in the Kermanshah region, west-central Zagros, Iran. Antiquity 91, 1-7.

Higham T., Brock F., Peresani M., Broglio A., Wood R., Douka K., 2009a. Problems with radiocarbon dating the Middle to Upper Palaeolithic transition in Italy. Quaternary Sci. Rev. 28, 1257-1267.

Higham T.F.G, Barton H., Turney C.S., Barker G., Ramsey C.B., Brock F., 2009b. Radiocarbon dating of charcoal from tropical sequences: Results from the Niah Great Cave, Sarawak, and their broader implications. J. Quaternary Sci. 24, 189-197.

Higham, T., Douka, K., Wood, R., Ramsey, C.B., Brock, F., Basell, L., Camps, M., Arrizabalaga, A., Baena, J., Barroso-Ruíz, C., Bergman, C., 2014. The timing and spatiotemporal patterning of Neanderthal disappearance. Nature 512, 306-309.

Hole F., Flannery K.V., 1968. The prehistory of southwestern Iran: A preliminary report. Proc. Prehis. Soc. 33, 147-206.

Hublin J.J., 2009. Out of Africa: Modern human origins special feature: The origin of Neandertals. Proc. Natl. Acad. Sci. 106, 16022-16027.

Jaubert, J., Biglari, F., Bordes, J.G., Bruxelles, L., Mourre, V., Shidrang, S., Naderi, R., Alipour, S., 2006. New research on Paleolithic of Iran: preliminary report of 2004 Iranian-French joint mission. Archaeol. Rep. 4, 17-26.

Jimenez-Espejo, F.J., Martínez-Ruiz, F., Finlayson, C., Paytan, A., Sakamoto, T., Ortega-Huertas, M., Finlayson, G., Iijima, K., Gallego-Torres, D., Fa, D., 2007. Climate forcing and Neanderthal extinction in Southern Iberia: Insights from a multiproxy marine record. Quaternary Sci. Rev. 26, 836-852.

Klein R.G., 1995. Anatomy, behavior, and modern human origins. J. World Prehist. 9, 167-198.

Marean C.W., Kim S.Y., 1998. Mousterian large-mammal remains from Kobeh Cave behavioral implications for Neanderthals and early modern humans. Curr. Anthropol. 39, S79-S114.

Mellars P., 1989. Major issues in the emergence of modern humans. Curr. Anthropol. 30, 349-385.

Mellars P., 1991. Cognitive changes and the emergence of modern humans in Europe. Cambridge Archaeol. J. 1, 63-76.

Olszewski D.I., Dibble H.L., 1994. The Zagros Aurignacian. Curr. Anthropol. 35, 68-75.

Otte, M., Kozłowski, J.K., 2004. La place du Baradostien dans l'origine du Paléolithique supérieur d'Eurasie. L'anthropologie 108, 395-406.

Otte, M., Biglari, F., Flas, D., Shidrang, S., Zwyns, N., Mashkour, M., Naderi, R., Mohaseb, A., Hashemi, N., Darvish, J., Radu, V., 2007. The Aurignacian in the Zagros region: New research at Yafteh Cave, Lorestan, Iran. Antiquity 81, 82-96.

Otte, M., Shidrang, S., Zwyns, N., Flas, D., 2011. New radiocarbon dates for the Zagros Aurignacian from Yafteh cave, Iran. J. Hum. Evol. 61, 340-346.

Prüfer, K., Racimo, F., Patterson, N., Jay, F., Sankararaman, S., Sawyer, S., Heinze, A., Renaud, G., Sudmant, P.H., De Filippo, C., Li, H., 2014. The complete genome sequence of a Neanderthal from the Altai Mountains. Nature 505, 43-49.

Richards M.P., Trinkaus E., 2009. Isotopic evidence for the diets of European Neanderthals and early modern humans. Proc. Natl. Acad. Sci. 106, 16034-16039.

Rosenberg M., 1985. Report on the 1978 sondage at Eshkaft-e Gavi. Iran. 23, 51-62.

Schlanger N., 1996. Understanding Levallois: Lithic technology and cognitive archaeology. Cambridge Archaeol. J. 6, 231-254.

Scott J.E., Marean C.W., 2009. Paleolithic hominin remains from Eshkaft-e Gavi (southern Zagros Mountains, Iran): Description, affinities, and evidence for butchery. J. Hum. Evol. 57, 248-259.

Solecki R.S., 1955. Shanidar Cave, a Paleolithic site in northern Iraq. In: Annual Report of the Board of Regents of the Smithsonian Institution, Publication 4190. United States Government Printing Office, pp. 389-426.

Solecki R.S., 1957. Shanidar Cave. Sci. Am. 197, 58-64.

Solecki R.S., 1960. Three adult Neanderthal skeletons from Shanidar Cave, northern Iraq. In: Annual Report of the Board of Regents of the Smithsonian Institution, Publication 4392. United States Government Printing Office, pp. 603-35.

Solecki R.S., 1963. Prehistory in Shanidar valley, northern Iraq. Science 139, 179-193.

Solecki R.S., 1975. Shanidar IV, a Neanderthal flower burial in northern Iraq. Science 190, 880-881.

Solecki R.S., Solecki R.L., 1993. The pointed tools from the Mousterian occupations of Shanidar Cave, northern Iraq. In: Olszewski D., Dibble H. (Eds.), The Paleolithic Prehistory of the Zagros-Taurus. The University Museum of Archaeology and Anthropology, University of Pennsylvania, Philadelphia, pp. 119-146.

Stuiver, M. and H. A. Polach. 1977. Discussion: Reporting of C-14 data. Radiocarbon 19, 355-363.

Trinkaus E., 1978. Dental remains from the Shanidar adult Neanderthals. J. Hum. Evol. 7, 369-382.

Trinkaus E., Zimmerman M., 1982. Trauma among the Shanidar Neandertals. Am. J. Phys. Anthropol. 57, 61-76.

Vahdati Nasab H.V., 2011. Paleolithic archaeology in Iran. The International Journal of Humanities of the Islamic Republic of Iran 18, 63-87.

Vahdati Nasab H.V., Clark G.A., Torkamandi S., 2013. Late Pleistocene dispersal corridors across the Iranian plateau: A case study from Mirak, a Middle Paleolithic site on the northern edge of the Iranian central desert (Dasht-e Kavir). Quatern. Int. 300, 267-281.

White, R., Arts, N., Bahn, P.G., Binford, L.R., Dewez, M., Dibble, H.L., Fish, P.R., Gamble, C., Meiklejohn, C., Ohel, M.Y., Pfeiffer, J., 1982. Rethinking the Middle/Upper Paleolithic transition [and comments and replies]. Curr. Anthropol. 23, 169-192.

Wood, R., Douka, K., Boscato, P., Haesaerts, P., Sinitsyn, A., Higham, T., 2012. Testing the ABOx-SC method: Dating known-age charcoals associated with the Campanian Ignimbrite. Quat. Geochronol. 9, 16-26.

Wood, R.E., Arrizabalaga, A., Camps, M., Fallon, S., Iriarte-Chiapusso, M.J., Jones, R., Maroto, J., de la Rasilla, M., Santamaría, D., Soler, J., Soler, N., Villaluenga, A., Higham, T.F.G., 2014. The chronology of the earliest Upper Palaeolithic in northern Iberia: New insights from L'Arbreda, Labeko Koba and La Viña. J. Hum. Evol. 69, 91-109.

**Supplementary Online Material**

OxCal 4.3 CQL code for Figure 5. Bayesian age model (Ghar-e Boof)

```
Plot()
 {
  Outlier_Model("General",T(5),U(0,4),"t");
  Sequence("Ghār-e Boof - Upper Palaeolithic")
  {
   Boundary("Start AH IV");
   Phase("AH IV")
   {
    R_Date("Find 209.2", 36030, 427)
    {
     color="green";
     Outlier("General", 0.05);
    };
    R_Date("Find 209.1", 33060, 296)
    {
     color="green";
     Outlier("General", 0.05);
    };
    R_Date("OxA-32390", 31620, 180)
    {
     Outlier("General", 0.05);
     color="blue";
```

```
  };
 };
 Boundary("End AH IV/Start AH IIIb");
 Phase("AH IIIb")
 {
  R_Date("Find 172", 34900, 600)
  {
   color="green";
   Outlier("General", 0.05);
  };
 };
 Boundary("End AH IIIb/Start AH III");
 Phase("AH III")
 {
  R_Date("Find 156", 31150, 490)
  {
   color="green";
   Outlier("General", 0.05);
  };
  R_Date("OxA-X-2633-54", 35950, 800)
  {
   Outlier("General", 0.05);
   color="blue";
  };
 };
 Boundary("End AH III");
};
};
```

OxCal 4.3 code for Figure 7. Bayesian age model (Yafteh Cave)

```
Plot()
```

```
{
 Outlier_Model("General",T(5),U(0,4),"t");
 Sequence("Yafteh Cave")
 {
  Boundary("Start Boundary");
  Sequence("Upper Palaeolithic")
  {
   R_Date("Beta-245912", 34160, 360)
   {
    Outlier("General", 0.05);
   };
   R_Date("Beta-245911", 33520, 330)
   {
    Outlier("General", 0.05);
   };
   R_Date("Beta-245907", 32770, 290)
   {
    Outlier("General", 0.05);
   };
   R_Date("Beta-245913", 34360, 340)
   {
    Outlier("General", 0.05);
   };
   R_Date("Beta-251061", 31120, 240)
   {
    Outlier("General", 0.05);
   };
   R_Date("Beta-245909", 33330, 310)
   {
    Outlier("General", 0.05);
   };
   R_Date("Beta-245844", 35450, 600)
```

```
{
 Outlier("General", 0.05);
};
R_Date("Beta-245908", 33430, 310)
{
 Outlier("General", 0.05);
};
R_Date("Beta-251060", 33260, 300)
{
 Outlier("General", 0.05);
};
R_Date("Beta-251059", 32900, 290)
{
 Outlier("General", 0.05);
};
R_Date("Beta-251062", 33160, 240)
{
 Outlier("General", 0.05);
};
R_Date("Beta-251058", 32190, 290)
{
 Outlier("General", 0.05);
};
R_Date("Beta-245910", 33800, 330)
{
 Outlier("General", 0.05);
};
R_Date("Beta-206712", 33400, 840)
{
 Outlier("General", 0.05);
};
R_Date("Beta-206711", 24470, 280)
```

```
   {
    Outlier("General", 0.05);
   };
  };
  Boundary("End Boundary");
 };
};
```

OxCal 4.3 code for Figure 8. Bayesian age model (Shanidar Cave)

```
Plot()
{
 Outlier_Model("General",T(5),U(0,4),"t");
 Sequence("Shanidar Cave")
 {
  Boundary("Start Layer D");
  Phase("Layer D")
  {
   R_Date("GRO-2527", 46900, 1500)
   {
    Outlier("General", 0.05);
   };
   R_Date("GrN-1495", 50600, 3000)
   {
    Outlier("General", 0.05);
   };
  };
  Boundary("End D/Start C");
  Sequence("Layer C")
  {
   Phase("Base Level")
   {
```

```
 R_Date("GRO-2549", 35080, 500)
 {
  Outlier("General", 0.05);
 };
 R_Date("GrN-2015", 34540, 500)
 {
  Outlier("General", 0.05);
 };
 R_Date("GrN-2016", 35440, 600)
 {
  Outlier("General", 0.05);
 };
 R_Date("GrN-1494", 34000, 420)
 {
  Outlier("General", 0.05);
 };
 R_Date("GrN-1830", 33900, 900)
 {
  Outlier("General", 0.05);
 };
};
Phase("Upper Level")
{
 R_Date("W-650", 33300, 1000)
 {
  Outlier("General", 0.05);
 };
 R_Date("W-178", 29500, 1500)
 {
  Outlier("General", 0.05);
 };
 R_Date("W-654", 28700, 700)
```

```
    {
     Outlier("General", 0.05);
    };
   };
  };
  Boundary("End sterile layer/Start C");
  Boundary("End B/Start sterile layer");
  Sequence("Layer B")
  {
   Phase("Layer B2")
   {
    R_Date("W-179", 12000, 400)
    {
     Outlier("General", 0.05);
    };
   };
   Phase("Layer B1")
   {
    R_Date("W-667", 10600, 300)
    {
     Outlier("General", 0.05);
    };
   };
  };
  Boundary("End Layer B");
 };
};
```